

RF over fiber system for 5G application

Rana Salah Imarah¹ and Syamsuri Yaakob^{1,*}

¹Department of Computer and Communication Systems Eng. Faculty of Eng, University Putra Malaysia (UPM), Serdang, Selangor, Malaysia

*Corresponding author: syamsuri@upm.edu.my

Keywords

Optical carrier suppression modulation (OCS)

Optical millimeter-wave (MMW)

Dual-drive Mach-Zehnder modulator (DD-MZM)

Radio-over-Fiber (RoF) system

Article History

Received: 12 May 2022

Accepted: 4 July 2022

Published: 30 Dec 2022

Abstract

5G communications involve the transfer of several Gb/s information in their small cells. The main solutions for high-speed data transfers for this objective are millimeter-wave RF signals. It is difficult to produce these high-frequency RF signals on the electrical field, so more study is given to the photonic generation of these signals. In this study, the utilization of a dual-drive Mach-Zehnder Modulator (DD-MZM) illustrates a special optical millimeter-wave (MMW) generation. A new method for producing a local oscillator frequency quadrupling optical carrier suppression (OCS) MMW signal utilize two equivalent DD-MZMs based on this form is shown. Data flow on a Radio over Fiber (RoF) network for transmission and generation of a 2.5 Gbps downlink, at OSSR (Optical Sideband Suppression Ratio) of up to 32 dB is acquired by simulation. The Radio Frequency Spurious Suppression Ratio (RFSSRR) is 22 dB.

1. Introduction

The visibility for 5G is spacious, yet one side is fiber—such as connections to mobile devices that provide multi-gigabit data rates per second. Such technology will make many applications and services available, such as 3D telepresence and virtual reality, however, these high-capacity technologies would require mastery of the millimeter-wave spectrum to mobile applications within frequency bands over 24 GHz. Actually, cellular communications systems make full use of the accessible frequency below 4 GHz and, by their so nature, this frequency can only offer an extreme, 4 GHz bandwidth, even if they were all net for use, which is clearly not possible. Much wider bandwidths are possible by having a 5G millimeter-wave functionality, and several candidate millimeter bands are being considered for this type of service allocation and various constraint millimeter bands are existence considered to this form of service allocation [1].

The spectrum of millimeter waves is the spectrum band between (30 GHz - 300 GHz). Located between infrared waves and microwaves, this spectrum can also be utilized together with a recent 802.11ad Wi-Fi standard (operating at 60 GHz) for high-speed wireless communications. In addition, Fiber-optic connectivity sport an important part in the fronthaul and backhaul networks to enable the mixture of small cells and mm-wave radio for potential 5G modification.

To meet the planned 5G rollout targets by 2020, the optical access network (OAN) needs scalability: 1–10 Gb/s at the consumer terminal; 100 Gb/s for the backhaul truck; 1 Tb/s for the subway transmission and 1 Pb/s for the main transportation. However, Millimetre-wave Radio over Fiber (ROF) is the technology that has emerged as a competitive candidate capable of meeting the rising demands of broadband multimedia wireless users. The ROF a promising implementation solution to wireless or optical systems has attracted a great deal of attention due of its importance in providing wireless broadband access with improved access network ability and mobility and reduced system costs. Optical mm-wave generation is the main method from high transmission performance ROF systems [2]. The optical generation of MMW use an external modulator focused on OCS modulation is favoured between these modulation techniques due it can produce low spectral density, high sensitivity to the receiver, and low bandwidth request for RF signals [3]. Recently, several different approaches were suggested to produce an mm-wave signal. By utilize two cascaded MZMs, a 60 GHz MMW signal is generated [4]. To strip the optical carrier, it is necessary to use a Bragg grating filter (BGF) which leads to a large degradation of efficiency. A novel approach is proposed in [4] to produce an OCS MMW signals using a DD-MZM. Moreover, the optical MMW's repeated frequency is only double the frequency of the drive. Therefore, the generation of the 60 GHz OCS MMW signal requires expensive electrical devices. Throughout this paper, utilizing two analogous DD-MZMs, we propose a simple scheme for producing an OCS MMW signal. At the minimum transmission bias point (MITBP) at 90° two analogous DD-MZMs (MZ-up, MZ-down) are biased to support a broad variety of new application 5G scenarios like (EMBB).

Section 2 describes the layout of the process followed up by the simulation as defined in Section 3. Finally, the outcome is presented in Section 4.

2. System design

The transmitter portion is designed as one of the vital components in the modeling of the mm-wave ROF system. Using two parallel DD-MZMs, a simple scheme for generating an (OCS MMW) signal is proposed in this method. Two equivalent DD-MZMs (up and down) are based on the least transmission bias level (MITBP) together with 90° phase shift. The IDP-MZM modulates a continuous-wave (CW) generated by a distributed-feedback laser diode (DFB-LD), separated by a 3-dB optical splitter into 2 divisions, i.e. I and II. The two optical carriers of the section are then merged into 2 DD-MZMs. The branch I DD-MZM is referred to as MZ-up, while Branch II is referred to as MZ-down. Two second-order sidebands are shaped and maximized in the proposed quadruple frequency MMW generation scheme and the frequency distance between them is 60 GHz. In addition, The MZM (MZ-c) modulates the two sidebands of the second order with an ER of 30 dB with a baseband signal of 2.5 Gbps. The simulation was performed over 0 km (back to back) at a rate of 2.5 Gbps. The output signal from CS is amplified at the base station (BS) by the erbium-doped fiber amplifier (EDFA) which is used to recompense for the modulator's enrollment loss and is sent to the RAU via a 20 km SMF. Then, PD detects the quadrilateral frequency optical MMW, while the electrical Gaussian 1st-order band pass filter based at 60 GHz filters out the RF harmonics. To de-modulate the 2.5 Gbps signal of the created 60 GHz MMW signal, a mixer, a 60 GHz RF oscillator. And the electrical low pass filter together with a bandwidth of 2.5 GHz is used.

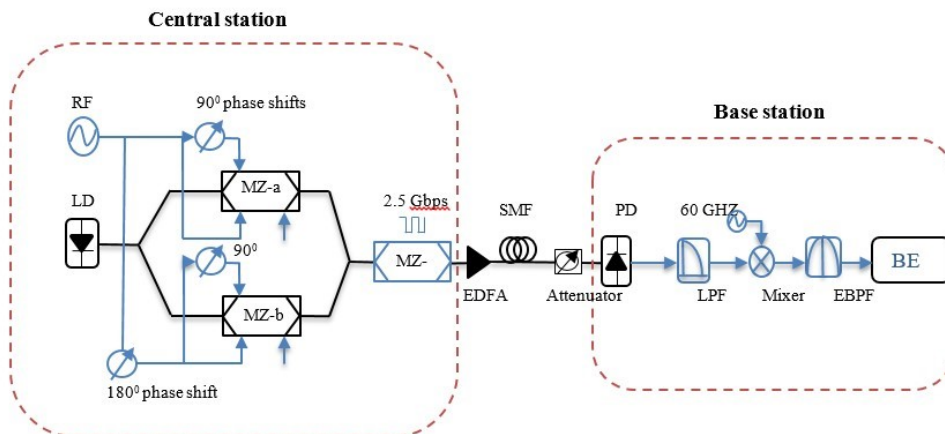


Figure 1. Schematic diagram of the OCS RoF setup.

3. Theoretical analysis

Parallel DD-MZMs have eight inputs called RF1, RF2, VDC1, and VDC2 for MZ-up and RF3, RF4, VDC3, and VDC4 for MZ-down. RF1 and RF2 represents the input RF driving signals applied to each MZ-up drive electrode with 90° phase difference. RF3 and RF4 represents the input RF driving signals applied to each MZ-down drive electrode with 90° phase difference. VDC1 and VDC2 represents the DC bias voltages applied to MZ-up bias electrodes. VDC3 and VDC4 represents the DC bias voltages applied to MZ-down bias electrodes. A 180° phase shift is introduced between the RF driving signals applied to MZ-up and MZ-down, i.e., the DC bias voltage consisting of VDC2 and VDC4 is set to V_π . The other DC bias voltage consisting of VDC1 and VDC3 is set to 0 V. A 90° phase shift is introduced between the RF driving signals applied to the MZ-up and MZ-down drive electrodes. Thus, the RF driving signals applied to the four RF electrodes of the two DD-MZMs are $V_{RF}\cos(W_{RF}t + \frac{\pi}{2})$, $V_{RF}\cos(W_{RF}t)$, $V_{RF}\cos(W_{RF}t + \frac{\pi}{2})$, and $V_{RF}\cos(W_{RF}t)$. The output of MZ-up contains all nth order optical sidebands, except for $n=4k$, where k is an integer. The proposed 60 GHz MMW generation scheme based on two parallel DD-MZMs is shown schematically in Fig. 1. The CW generated from a DFB-LD can be expressed as:

$$E_{in}(t) = E_0 \exp(j\omega_0 t) \tag{1}$$

The voltage of the RF-driven signal applied to MZ-up and MZ-down is:



$$V_{RF}t = V_{RFCOS}(W_{RF}t) \tag{2}$$

where E_0 and V_{RF} are the signal amplitudes and w_0 and w_{RF} are the angular frequency of the CW and the RF oscillator signal, respectively. MZ-up and MZ-down both biased at the MITBP. A phase shift 180° is introduced between the RF driving signals on MZ-up and MZ-down. If the ER of the two DD-MZMs is assumed to be infinite, i.e., ideal condition, the output field of the optical coupler (OC) can mathematically write as:

$$E_{out}(0, t) = E_I(0, t) + E_{II}(0, t) \tag{3}$$

where $E_I(0, t)$ is the optical field exported from MZ-up defined as:

$$\begin{aligned} E_I(0, t) &= \frac{E_0}{4} e^{jw_0t} [e^{j\frac{\pi}{V_\pi} V_{RFCOS}(w_{RF}t + \frac{\pi}{2})} + e^{j\frac{\pi}{V_\pi} V_{RFCOS}(w_{RF}t + \frac{\pi}{2})} \cdot e^{j\frac{V_{DC2}}{V_\pi} \pi}] \\ &= \frac{E_0}{4} e^{jw_0t} [e^{j\frac{\pi}{V_\pi} V_{RFCOS}(w_{RF}t + \frac{\pi}{2})} + e^{j\frac{\pi}{V_\pi} V_{RFCOS}(w_{RF}t + \frac{\pi}{2})} \cdot e^{j\pi}] \\ &= \frac{E_0}{4} e^{jw_0t} [e^{j\frac{\pi}{V_\pi} V_{RFCOS}(w_{RF}t + \frac{\pi}{2})} - e^{j\frac{\pi}{V_\pi} V_{RFCOS}(w_{RF}t + \frac{\pi}{2})}] \end{aligned} \tag{4}$$

By applying the Jacobi–Anger expansion to Eq. 4, $E_I(0, t)$ can be written as:

$$\begin{aligned} E_I(0, t) &= \frac{E_0}{4} e^{jw_0t} [\sum_{n=-\infty}^{\infty} j^n j_n(m) e^{jn(w_{RF}t + \frac{\pi}{2})} - \sum_{n=-\infty}^{\infty} j^n j_n(m) e^{jn(w_{RF}t)}] \\ &= \frac{E_0}{4} e^{jw_0t} [\sum_{n=-\infty}^{\infty} j_n(m) e^{j(nw_{RF}t + n\pi)} - \sum_{n=-\infty}^{\infty} j_n(m) e^{j(nw_{RF}t + n\frac{\pi}{2})}] \\ &= \frac{E_0}{4} e^{jw_0t} [\sum_{n=-\infty}^{\infty} j_n(m) e^{j(nw_{RF}t + \frac{3n\pi}{4} + \frac{n\pi}{4})} - \sum_{n=-\infty}^{\infty} j_n(m) e^{j(nw_{RF}t + \frac{3n\pi}{4} + \frac{n\pi}{4})}] \\ &= \frac{E_0}{2} [\sum_{n=-\infty}^{\infty} j_n(m) \sin \frac{n\pi}{4} \cdot e^{j(w_0 + nw_{RF}t + \frac{3n\pi}{4})}] \end{aligned} \tag{5}$$

where V_π is the switching voltage of MZM, m is the RF modulation index defined as $m = V_{RF} \cdot \frac{n}{V_\pi}$ and j_n is the n th-order Bessel function of the first kind. Equation 5 indicates that the $(4n)$ th-order optical sidebands are eliminated because of the term $\sin(\frac{n\pi}{4})$. The optical field at the output of MZ-down can mathematically be written as:

$$\begin{aligned} E_I(0, t) &= \frac{E_0}{4} e^{jw_0t} [e^{j\frac{\pi}{V_\pi} V_{RFCOS}(w_{RF}t + \frac{\pi}{2})} + e^{j\frac{\pi}{V_\pi} V_{RFCOS}(w_{RF}t + \pi)} \cdot e^{j\frac{V_{DC2}}{V_\pi} \pi}] \\ &= \frac{E_0}{4} e^{jw_0t} [e^{j\frac{\pi}{V_\pi} V_{RFCOS}(w_{RF}t + \frac{3\pi}{2})} + e^{j\frac{\pi}{V_\pi} V_{RFCOS}(w_{RF}t + \pi)} \cdot e^{j\pi}] \\ &= \frac{E_0}{4} e^{jw_0t} [e^{jmc\cos(w_{RF}t + \frac{3\pi}{2})} - e^{jmc\cos(w_{RF}t + \pi)}] \\ &= \frac{E_0}{4} e^{jw_0t} [\sum_{n=-\infty}^{\infty} j^n J_n(m) e^{jn(w_{RF}t + \frac{3\pi}{2})} - \sum_{n=-\infty}^{\infty} j^n J_n(m) e^{jn(w_{RF}t + \pi)}] \\ &= \frac{E_0}{4} e^{jw_0t} [\sum_{n=-\infty}^{\infty} J_n(m) e^{j(nw_{RF}t + \frac{3\pi}{2} + \frac{n\pi}{2})} - \sum_{n=-\infty}^{\infty} J_n(m) e^{j(nw_{RF}t + n\pi + n\frac{\pi}{2})}] \\ &= \frac{E_0}{2} [\sum_n J_n(m) \sin(\frac{n\pi}{4}) \cdot e^{j[(w_0 + nw_{RF})t + \frac{n\pi}{4}]}] \end{aligned} \tag{6}$$

Thus, the output field of the OC can be expressed as:



$$\begin{aligned}
 E_{out}(0, t) &= E_I(0, t) + E_{II}(0, t) \\
 &= \frac{E_0}{2} \left(\left[\sum_{n=-\infty}^{\infty} J_n(m) \sin\left(\frac{n\pi}{4}\right) \cdot e^{j[w_0 + nw_{RF}t + \frac{3n\pi}{4}]} \right] + \left[\sum_{n=-\infty}^{\infty} J_n(m) \sin\left(\frac{n\pi}{4}\right) \cdot e^{j[w_0 + nw_{RF}t - \frac{n\pi}{4}]} \right] \right) \quad (7) \\
 &= E_0 \left[\sum_{n=-\infty}^{\infty} J_n(m) \sin\left(\frac{n\pi}{4}\right) \cdot \cos\left(\frac{n\pi}{4}\right) e^{j[w_0 + nw_{RF}t - \frac{n\pi}{4}]} \right]
 \end{aligned}$$

Equation 7 indicates that the n th-order sidebands are all eliminated, excluding $n = 4k - 2$, where k is an integer. Equation 7 also shows that the $(4k - 2)$ th-order sidebands interfere constructively and that the odd-order sidebands destructively interfere at the output of the OC. This is because the 180° phase shift between the RF driving signals applied to the two MZMs which makes the polarities of the odd-order sidebands at the output of MZ-up to be in opposition to those at the output of MZ-down.

When generated optical MMW signals are transmitted over Z -length downlink fiber to the base station (BS), the two second-order sidebands will have various group velocities due to the fiber chromatic dispersion. The desired quadruple-frequency MMW signal is detected by using a PD, and the complex amplitude of its photodetector current can be written as:

$$\begin{aligned}
 I_{4w_{RF}}(Z, t) &= \mu [E(Z, t)]^2 \\
 &= \mu [E(Z, t) \cdot E(Z, t)^*] \\
 &= E_0^2 \alpha^2 e^{-2\gamma z} J_2^2(m) \mu \left(\left(e^{j[(w_0 - 2w_{RE})t - \beta(w_0 - zw_{RE})Z]} \cdot e^{-j\frac{\pi}{2}} - e^{j[(w_0 + 2w_{RE})t - \beta(w_0 + zw_{RE})Z]} \cdot e^{+j\frac{\pi}{2}} \right) \right. \quad (8) \\
 &\quad \left. \left(e^{-j[(w_0 + 2w_{RE})t - \beta(w_0 + zw_{RE})Z]} \cdot e^{-j\frac{\pi}{2}} - e^{-j[(w_0 - 2w_{RE})t - \beta(w_0 - zw_{RE})Z]} \cdot e^{+j\frac{\pi}{2}} \right) \right) \\
 &= 2E_0^2 \alpha^2 e^{-2\gamma z} J_2^2(m) \mu \{1 + \cos[4w_{RE}(t - \beta(w_0)Z)]\}
 \end{aligned}$$

where γ is the fiber loss, $\beta(2)$ is the propagation constant of the fiber and v_g denotes the group velocity. Equation 8 indicates that the amplitude of the current for the desired MMW signal at $4w_{RF}$ is independent of fiber dispersion.

4. Simulation and Results

In this section, the performance of the 60 GHz optical MMW signal is evaluated. A CW generated from the DFB-LD is sent at a central wavelength of 1552.52 nm to two IDP-MZM sub-MZMs with a linewidth of 10 MHz. Two comparable DD-MZMs with 4v switching voltage and 3 dB insertion loss. The two DDMZMs are paired by two optical couplers while the couplers' power-splitting ratio is 0.5. A 30 GHz RF LO drives MZ-up, while the same 180° RF LO drives MZ-down. Therefore, the RF guided signals are applied with separate phase shifts to the four arms of the two DDMZMs.

Figure 2a offers the simulated optical spectrum from the 60 GHz OCS MMW signal to the 0 km transmission distance while the two DD-MZMs' ER is infinite. It is therefore essentially composed of 2 strong second-order sidebands with a 60 GHz spacing to two feeble sixth-order 180 GHz spacing sidebands. The OSSR is 32 dB and the second-order sideband power are greater than the sixth order sideband power. Figure 2b displays the 60 GHz OCS MMW simulated optical spectrum when the ER of two of the DD-MZMs is 30 dB. Clearly the energy of the second-order optical sideband is the max, the OSSR is 30 dB.

The coveted frequency quadrupling 60 GHz mm-wave and false 120 GHz mm-wave signals are produced simultaneously due to the presence of the unwanted sixth-order sideband. However, the output of the 60 GHz mm-wave signal is more than in the 120 GHz mm-wave signal while, like shown in Figure 3, the RFSSRR (the energy ratio of the expected 60 GHz MMW signal to the erroneous 120 GHz MMW signal) is 22 dB.

4.1 The Eye Diagram

The eye diagram is one of the important diagrams in explaining the system performance. This diagram is capable of showing the existence of error, and the frequency of the harmonic or phase. Figure 4 displays the down-transform 2.5 Gbps electrical eye manner of the 60 GHz MMW after transportation through different fiber lengths. The eye

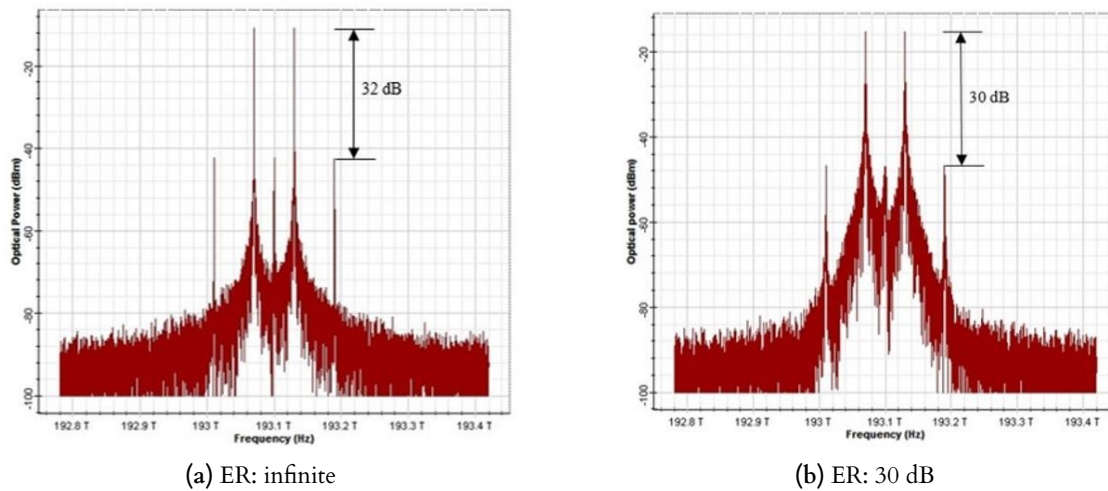


Figure 2. Simulated optical spectrum of the 60 GHz OCS MMW signal when the ER: (a) infinite and (b) 30 dB

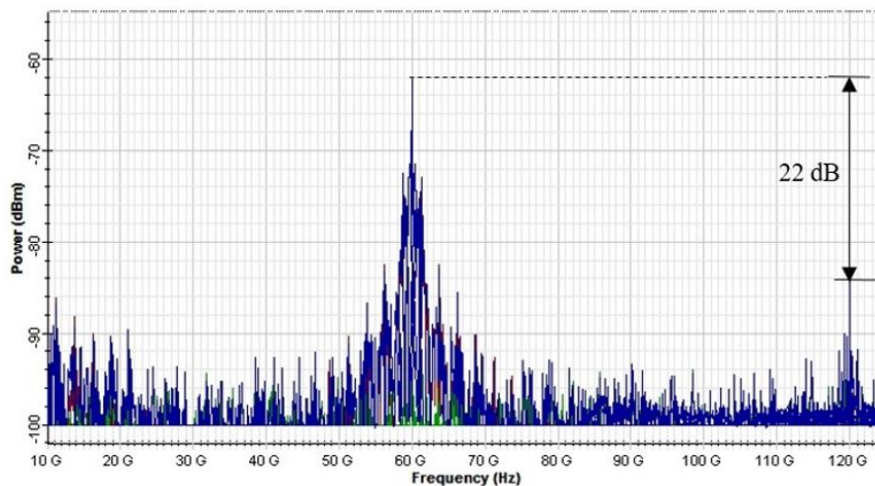


Figure 3. Simulated electrical spectrum of the 60 GHz MMW signal when the ER is 30 dB.

diagram of the received signal at 2 km can be seen to be completely clear and wide open. And, because of optical fiber weakness such as; chromatic dispersion and attenuation, eye diagrams start to be blurred when transmission distance to 50 km is increased. The eye diagrams obtained showed that eliminating the carrier provides advantages in transmitting the information more efficiently with the obtained mm-wave. Thus, the output of the MMW signal produced is therefore appropriate.

4.2 The Bit Error Rate (BER) performances

Figure 5 display a decrease of the BER value from (-5 to -20) as the level of optical power ρ rises from 0 dBm to 10 dBm.

Figure 6 indicates the down-converted BER curve of the demodulated 2.5 Gbps signal with specific transmission lengths from the 60 GHz MMW. It clearly shows that the BER rising as the fiber length raises. The graph indicates that the BER is less than 40 km negligible for the fiber length. When the effective light power is decreased to -5 dBm at 50 km transmission distance the system shows a high bit error rate value ($BER \geq 10^{-12}$). The longer fiber length will present a larger dispersion and attenuation, as well as increasing the BER, and suggests that the proposed method is better suited for data transmission between 1 and 40 km.

Figure 7 displays the minimum BER plot expressed as a function of the generated MMW signal's power received. The main benefit of the external modulation method suggested is the simple frequency tuning and its wide tuning range. The received power sensitivity is -12.8 and -12.1 dBm at the BER of 1×10^{-23} before and after 20 km transmission, respectively.

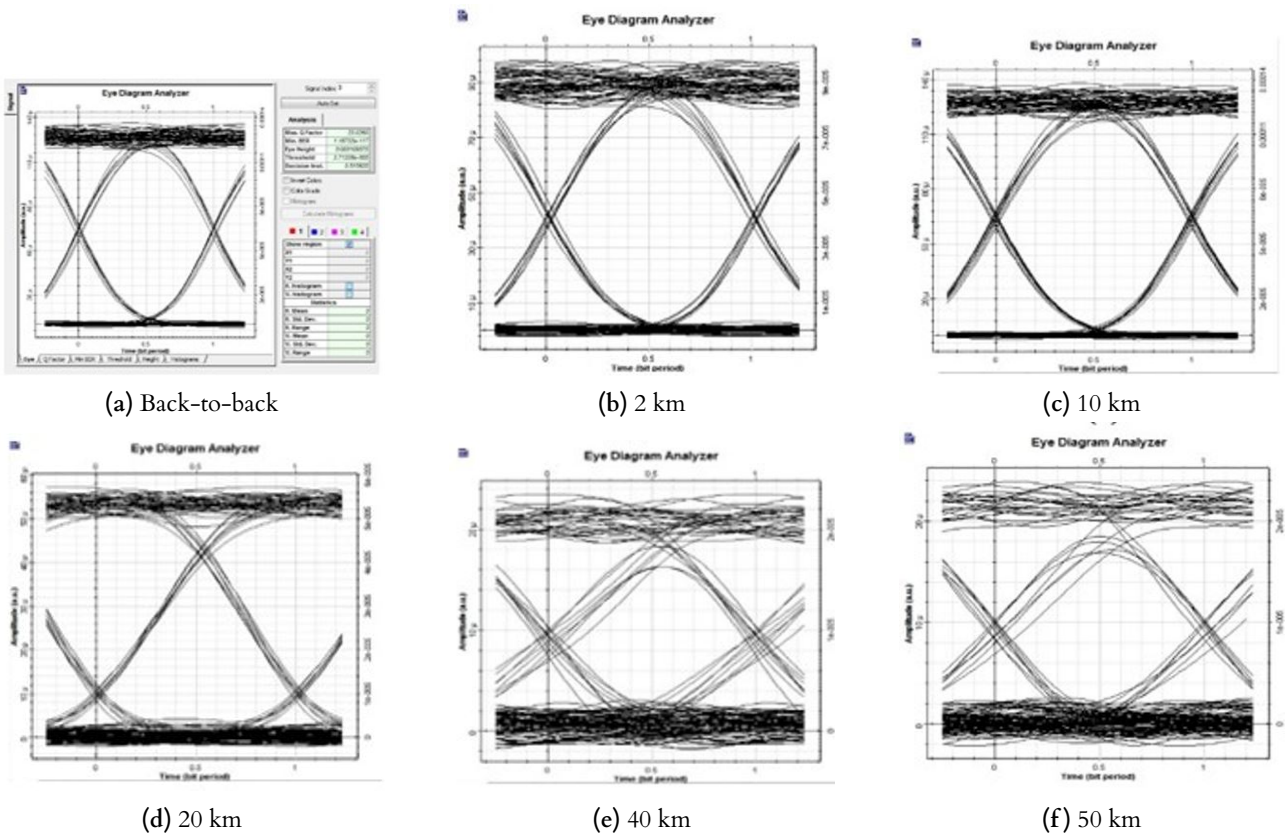


Figure 4. The eye patterns of the optical MMW by simulation at (a) back-to-back, (b) 2 km, (c) 10 km, and (d) 20 km, (e) 40 km, and (f) 50 km

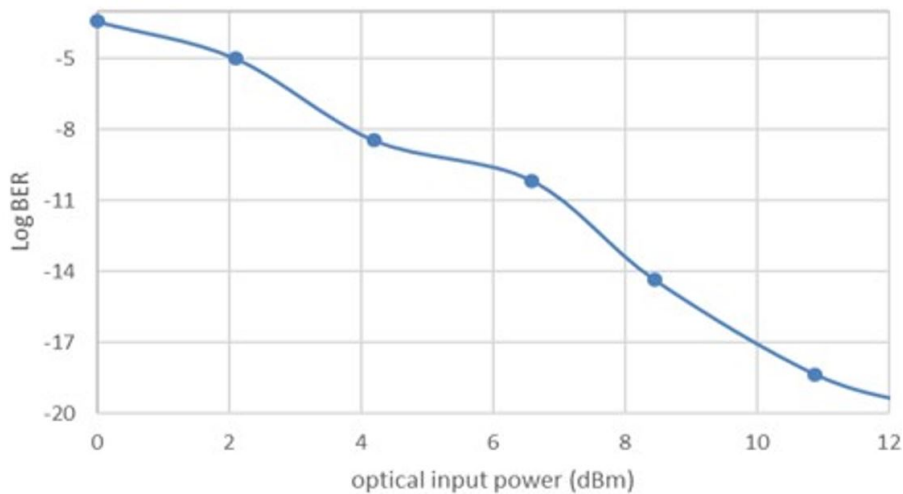


Figure 5. BER versus optical input power.

5. Conclusions

We have proposed in this paper an easy-to-implement scheme for generating and transmitting a 2.5 Gbps downlink flow in a 60 GHz RoF network through two commercial parallel DD-MZMs. The simulation results indicate that from a 30-GHz RF oscillator, a 60-GHz MMW signal can be generated. If the ER is 30 dB, OSSR is equal to 30 dB and the RFSSRR is equal to 22 dB. While the scheme used a broad modulation index to quadruple the frequency, it may decrease the intricacy of the central station, and its unit frequency requirement. It thus appears to be a possible solution to wireless communication networks with 60 GHz MMW.

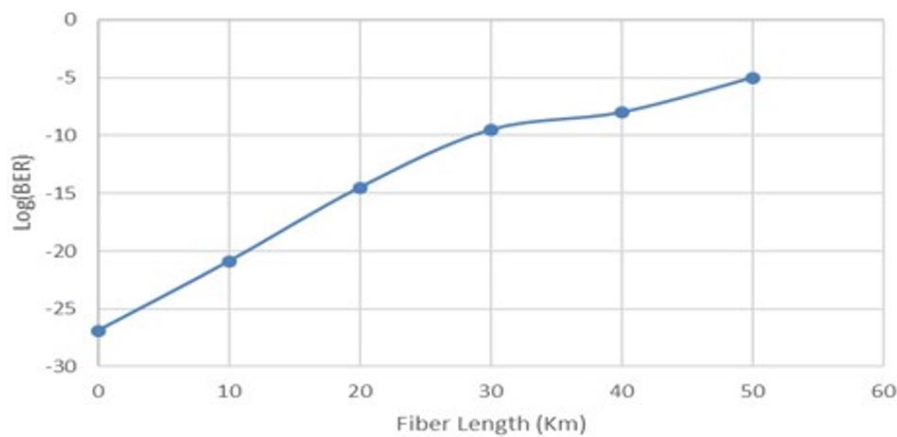


Figure 6. BER as a function of length of the fiber.

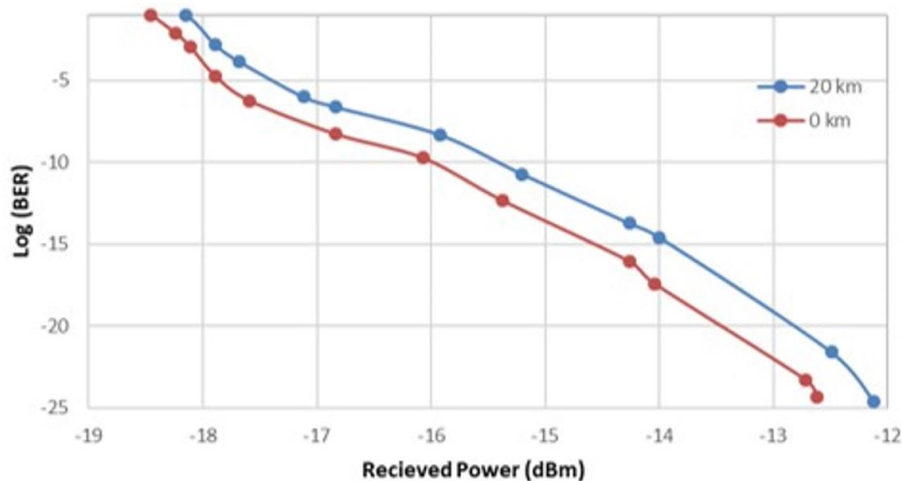


Figure 7. Plot for BER performance and received power for the proposed MMW signal.

References

- [1] C. Liu, M. Li, S. V. Hanly, P. Whiting, and I. B. Collings, "Millimeter-wave small cells: Base station discovery, beam alignment, and system design challenges," *IEEE Wireless Communications*, vol. 25, no. 4, pp. 40–46, Aug. 2018. doi: 10.1109/mwc.2018.1700392.
- [2] S. E. Alavi, M. R. K. Soltanian, I. S. Amiri, M. Khalily, A. S. M. Supa'at, and H. Ahmad, "Towards 5G: A photonic based millimeter wave signal generation for applying in 5G access fronthaul," *Scientific Reports*, vol. 6, no. 1, Jan. 2016. doi: 10.1038/srep19891.
- [3] T. S. Rappaport, S. Sun, R. Mayzus, *et al.*, "Millimeter wave mobile communications for 5G cellular: It will work!" *IEEE Access*, vol. 1, pp. 335–349, 2013. doi: 10.1109/access.2013.2260813.
- [4] Z. Kaleem, B. Hui, and K. Chang, "QoS priority-based dynamic frequency band allocation algorithm for load balancing and interference avoidance in 3GPP LTE HetNet," *EURASIP Journal on Wireless Communications and Networking*, vol. 2014, no. 1, Nov. 2014. doi: 10.1186/1687-1499-2014-185.